ISSN 0208-7774 TRIBOLOGIA 3/2021 p. 45–56
DOI: 10.5604/01.3001.0015.6898

Krzysztof WIERZCHOLSKI[*], Jacek GOSPODARCZYK[**]

ON RANDOM EXPECTED VALUES VARIATIONS OF TRIBOLOGY PARAMETERS IN HUMAN HIP JOINT SURFACES

O ZMIANACH LOSOWYCH WARTOŚCI PARAMETRÓW TRIBOLOGICZNYCH NA POWIERZCHNIACH STAWÓW BIODROWYCH CZŁOWIEKA

Key words: human hip joint, random load carrying capacity, friction forces, random synovial bio-fluid dynamic viscosity, stochastic expected values variations, phospholipids bilayer, analytical stochastic solutions, experimental measurements.

Abstract: This paper presents recent progress in the knowledge concerning the stochastic theory of bio- hydrodynamic lubrication with a phospholipids bilayer. On the basis of experimental measurements and analytical solutions, the research concerns the determination of the random expectancy values of load carrying capacity, the friction coefficient, and synovial fluid dynamic variations. After numerous measurements, it directly follows that the random density function of the gap height in the human joint usually indicates a disorderly increases and decreases in the height. Such irregular gap height variations have an important influence on the random synovial bio-fluid dynamic viscosity. This finally leads to the friction coefficient and cartilage wear changes of cooperating bio- surfaces. The main topic of this paper relates to the expectancy values of the tribology parameters localized inside the variable stochastic standard deviation intervals of the human joint gap height. The results obtained finally indicate the influence of the random roughness and growth of living biological cartilage surfaces on the expectancy values of the synovial fluid dynamic viscosity, load carrying capacity and friction forces in human hip joints.

Słowa kluczowe: staw biodrowy człowieka, losowa siła nośna, siły tarcia, losowa lepkość dynamiczna biocieczy, zmiany wartości oczekiwanych, dwuwarstwa fosfolipidów, losowe rozwiązania analityczne, pomiary eksperymentalne.

Streszczenie: Niniejsza praca przedstawia ostatnie osiągnięcia wiedzy w zakresie losowej teorii biohydrodynamicznego smarowania z udziałem fosfolipidów. Badania dotyczą losowych wartości oczekiwanych dla nośności, współczynników tarcia, zmian lepkości dynamicznej cieczy synowialnej, przeprowadzone na podstawie pomiarów doświadczalnych i obliczeń analitycznych. Z przeprowadzonych pomiarów doświadczalnych wynika, że losowa funkcja gęstości wysokości szczeliny w stawach człowieka wykazuje zazwyczaj nieprzewidywalne zmiany wysokości szczeliny. Takie nieregularne zmiany mają istotny wpływ na wartość lepkości cieczy biologicznej. Dlatego zmienia się współczynnik tarcia oraz zużycie biopowierzchni. Głównym celem pracy jest wyznaczenie losowej wartości oczekiwanej parametrów tribologicznych umiejscowionych wewnątrz zmiennego losowego przedziału odchylenia standardowego wysokości szczeliny stawu człowieka. Końcowe rezultaty uzyskane w pracy wykazują wpływ losowych chropowatości oraz wzrostu żywych powierzchni chrząstki stawowej na losowe wartości oczekiwane lepkości dynamicznej cieczy synowialnej, nośności, siły tarcia w stawie biodrowym człowieka.

[*] ORCID: 0000-0002-9074-4200. University of Economy (WSG), Garbary 2 Street, 85-229 Bydgoszcz, Poland, e-mail: krzysztof.wierzcholski@wp.pl.
[**] ORCID: 0000-0001-8248-9329. University of Economy (WSG), Garbary 2 Street, 85-229 Bydgoszcz, Poland, e-mail: jacek.gospodarczyk@byd.pl.

INTRODUCTION

The results of the latest numerous bio-tribology studies, carried out by means of an Atomic Force Microscope (AFM), have demonstrated that the PL (phospholipid) layer and random gap height variations fairly significantly control the course of the hydrodynamic lubrication of surfaces flown-around by biological fluids **[L. 1–2]**.

During the synovial fluid flow in the human hip joint gap, the cartilage superficial layer and the movable PL bilayer alters the gap height of the spherical human hip joint **[L. 3–5]**.

On the grounds of the latest numerous measurements performed by the AFM, it follows that the total gap height ε_T possesses random increments or decrements in comparison to the height of the nominal mean value **[L. 6]**.

The random gap height changes $\pm\delta_1$ can be caused indirectly by the following: random micro translations of cartilage and PL bilayer surfaces, non-continuous random loading and hydrodynamic pressure distribution p on the hip joint surfaces, various shapes of velocity distributions in the gap height direction of bio-fluid flow in the longitudinal direction of the gap, and stochastic changes in roughness geometry, or random and body growth of living cartilage cells (see **Fig. 1a, b, c, d**) **[L. 7**, **8, 9]**.

Analytical calculations and experimental measurements indicate **[L. 10**, **11]** that the random positive and negative changes in the joint gap height $\pm\delta_1$ have a direct and indirect impact on the stochastic synovial fluid dynamic viscosity presented in **Figs. 1a, b, c, d**. The direct influences are visible in analytical solutions presenting the

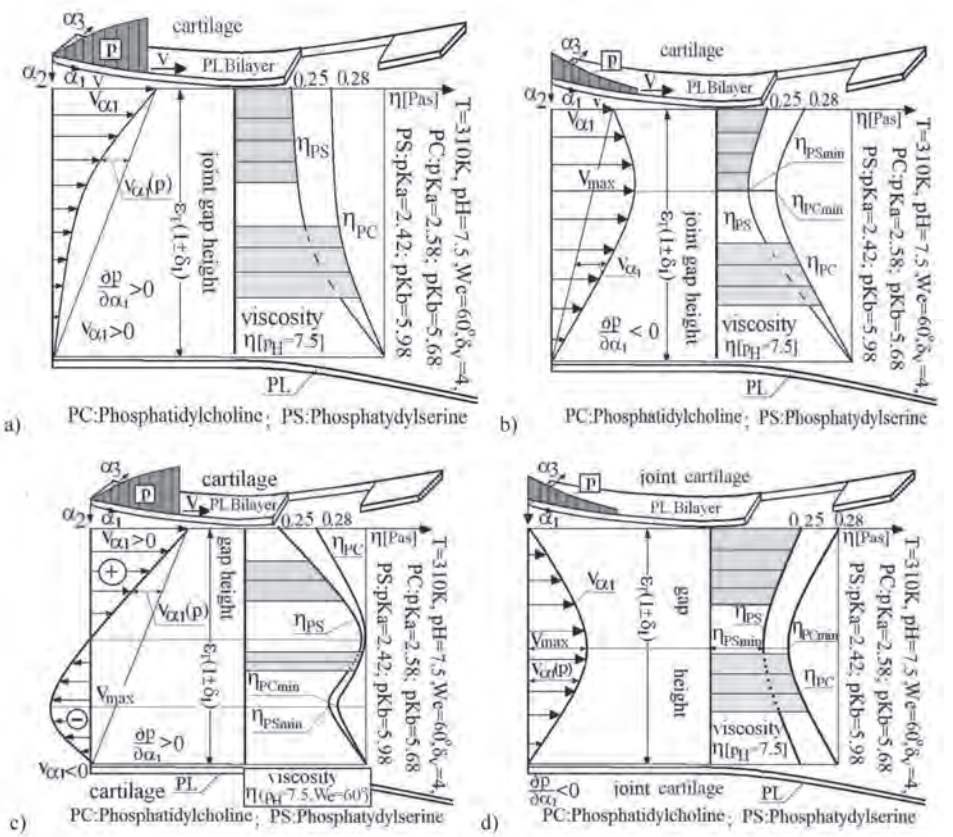

Fig. 1. a, b, c, d: illustration of direct influences of hydrodynamic pressure distributions p and cartilage surface translations on the synovial fluid velocity component distribution v_1 in circumferential $\alpha_1 = \varphi$ and longitudinal $\alpha_1 = \vartheta_1$ direction across the film thickness and an implication of these effects on the indirect impact of random joint gap height changes δ_1 associated with variations in dynamic viscosity distributions in the gap height direction $\alpha_2 = r$ between two cartilage surfaces in the spherical hip joint gap. We denote: PL – Phospholipid, PS – Phosphatidylcholine, PS – Phosphatidylserine

Rys. 1. a, b, c, d: ilustracja bezpośrednich wpływów rozkładu hydrodynamicznego ciśnienia p oraz przemieszczeń chrząstki na składową rozkładu prędkości cieczy synowialnej v_1 w obwodowym $\alpha_1 = \varphi$ oraz południkowym $\alpha_3 = \vartheta_1$ kierunku w poprzek grubości filmu wraz z implikacją tych efektów na pośredni wpływ zmian losowej wysokości szczeliny δ_1 powiązanej ze zmianami rozkładu lepkości dynamicznej η biocieczy w kierunku wysokości szczeliny $\alpha_2 = r$ pomiędzy dwiema powierzchniami sferycznymi stawu biodrowego

load carrying capacity and the fiction coefficient dependent on the gap height **[L. 12**, **13]**. It is evident that the indirect influences of the random gap height variations on the load carrying capacity are also provoked by stochastic changes in synovial fluid dynamic viscosity **[L. 14, 15]**.

The random increments (decrements) of the gap height imply decreases (increases) of the average velocity of synovial fluid in the joint gap, i.e. the share rate decreases (increases), respectively. Hence, for non-Newtonian fluid, it follows that the viscosity of synovial fluid increases (decreases). Finally, the load carrying capacity and friction coefficient depend strongly on synovial fluid viscosity.

The measurements presented in **Figs. 1a, b, c, d** are performed for the dimensional gap height $\varepsilon_T(\varphi,\vartheta_1) = 0.02$ mm limited by the nominally smooth biological movable surfaces. Calculation results are obtained for hydrogen ions concentration p_H = 7.5, for two kinds of lipids denoted by PC and PS, for the temperature of 310 K, cartilage wettability We = 60°, for non-Newtonian synovial fluid with nano lipid particles and collagen fibres concentration described by index $v_0\delta_v$ = 6.0 m/s, isoelectric point IP (We = 68°, synovial fluid dynamic viscosity η = 0.58 Pas) **[L. 16]**.

Figure 1a presents the case of an area where hydrodynamic pressure p is growing and the upper bio-surface that limits the gap is movable in the pressure growth direction. The lower surface is stationary. The velocities produced by the surface movement are smaller than the velocities generated by pressure p, whereas both velocities subtract mutually.

Figure 1b presents the case of an area where hydrodynamic pressure p is decreasing and the upper bio-surface that limits the gap is movable in the direction of the pressure decrease. The lower surface is stationary. Both velocities related to the pressure and the surface movement add mutually.

Figure 1c presents the case of an area where hydrodynamic pressure p is growing and the upper bio-surface that limits the gap is movable in the direction of the pressure increase. The lower surface is stationary. The velocities produced by the surface movement are greater than the velocities produced by pressure p, whereas both velocities subtract mutually.

Figure 1d presents the case of an area where hydrodynamic pressure p is decreasing and both bio-surfaces: the upper one and the lower one that limit the gap are motionless. Hence, there is only one parabolic distribution of the biofluid velocities produced by pressure p.

Based on the data depicted in **Figs. 1a, b, c, d**, it can be observed, among others, that the dynamic viscosity of the bio-fluid depends from the flow velocity, and dynamic viscosity is strongly connected with random gap height changes **[L. 4].** The places with the largest (smallest) flow velocity have the smallest (greatest) values of gap height changes; therefore, they possess the smallest (greatest) values of synovial fluid dynamic viscosity.

This paper focuses on direct and indirect influences of random gap height variations on the expected stochastic value of tribology parameters localization in the random standard interval of gap height variations between two cooperating cartilage spherical biological surfaces with a phospholipid bilayer in the human hip joint.

EXPECTED RANDOM GAP HEIGHT CONSTITUTION

The illustrations that describe the hip joint bonehead are elaborated in spherical coordinates: $(\alpha_1, \alpha_2, \alpha_3) = (\varphi,r,\vartheta)$, where $\alpha_1 = \varphi$ – circumferential direction, $\alpha_2 = r$ – radial direction, and $\alpha_3 = \vartheta$ – longitudinal direction of the sphere. The geometry of the human spherical hip joint and the PL bilayer sheet are presented in **Figs. 2a, b [L. 17, 4].**

Lubrication region Ω is defined by the following inequalities: $0 < \varphi < \pi$; $\pi R/8 < \vartheta < \pi R/2$, $\vartheta = \vartheta_1 R$, whereas R denotes the radius of the bonehead. The gap height in the hip joint between two nominal smooth spherical cartilage surfaces and deformed by the stochastic variations can be presented in the following dimensional form **[L. 5**, **18]**:

$$\varepsilon_T(\varphi,\vartheta_1,\delta_1) = \varepsilon_T(\varphi,\vartheta_1)\,[1+\delta_1(\varphi,\vartheta_1)] \equiv \varepsilon_0\varepsilon_{T1s}(\varphi,\vartheta_1)\,[1+\delta_1(\varphi,\vartheta_1)]. \quad (1)$$

The dimensional symbol $\varepsilon_T(\varphi,\vartheta_1,\delta_1)$ [m] describes the total gap height. Symbol $\varepsilon_{T1s}(\varphi,\vartheta_1)$ denotes the dimensionless gap height limited by the nominally smooth biological movable surfaces, ε_0 is the characteristic dimensional value of gap height. The expected value of the arbitrary random variable correction δ_1 and the expected dimensionless function of the total gap height is defined by the following expressions **[L. 4, 18]**:

$$EX(\delta_1) = \int_{-\infty}^{+\infty} (\delta_1) \times f(\delta_1) d\delta_1, \quad (2a)$$

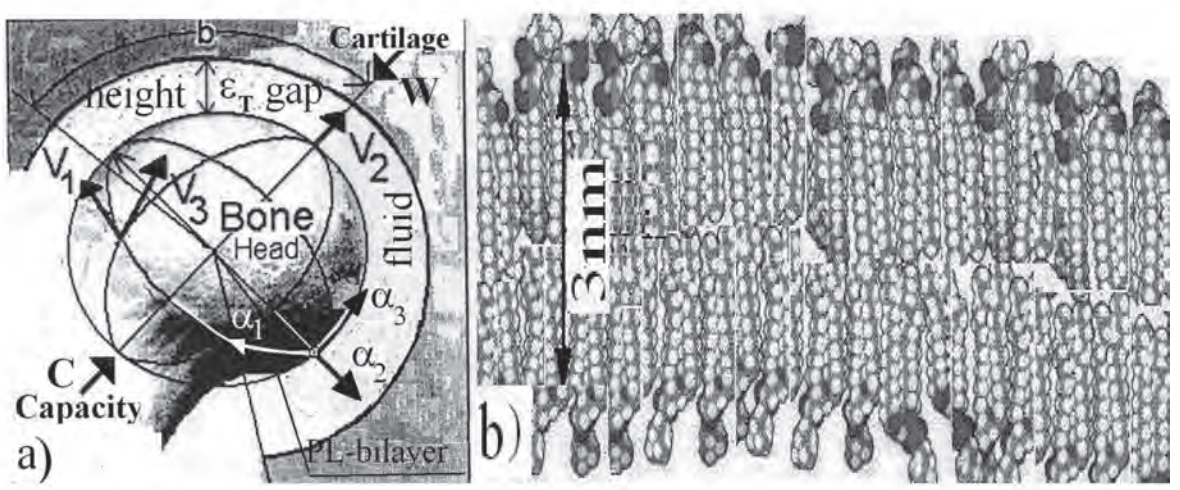

Fig. 2. Human hip joint gap height for random deformable cartilage surface: a) joint gap between hip bone head and sleeve (acetabulum), b) phospholipid (PL) bilayer sheet on internal sleeve surface

Rys. 2. Wysokość szczeliny stawu biodrowego dla losowo odkształcalnej powierzchni chrząstki stawowej: a) szczelina stawu pomiędzy głową stawu biodra i panewką, b) warstwa fosfolipidów na wewnętrznej powierzchni panewki

$$EX(\varepsilon_{T1}) = EX[\varepsilon_{T1s}(1+\delta_1)] = \varepsilon_{T1s}\left[1+EX(\delta_1)\right] = \varepsilon_{T1s}\left[1+\int_{-\infty}^{+\infty}(\delta_1)\times f(\delta_1)d\delta_1\right]. \tag{2b}$$

We denote: EX – expected operator, f – probability density function obtained from the measurements. Function f assigns probability P for variable random correction δ_1. Standard deviation σ, for random variable correction accepts the following known form **[L. 5, 18]**:

$$\sigma \equiv \sqrt{EX(\delta_1)^2 - EX^2(\delta_1)}. \tag{3}$$

The ordinate values of the probability density function f are the probabilities assigned to the positive or negative gap height correction values δ_1 in individual points on the joint gap height, and these are caused, among others, by the influences of cartilage transactions, pressure, and synovial fluid velocity distributions that are presented in **Fig. 1a, b, c, d.**

OUTLINE OF THEORETICAL AND NUMERICAL RESEARCH

The lubrication problem is described by the following equations: equilibrium of momentum equations, a continuity equation, an energy equation and a Young-Kelvin Laplace equation [**L. 4, 19]**. We take into account the following expected random functions [**L. 20]**: hydrodynamic pressure $EXp(\varphi, \vartheta)$, temperature $EXT(\varphi, r, \vartheta)$, synovial fluid velocity components $EXv_i(\varphi, r, \vartheta)$ for $i = \varphi, r, \vartheta$, the random dynamic viscosity of synovial fluid $EX\eta_T(\varphi, r, \vartheta)$, and random joint gap height $EX\varepsilon_T(\varphi, \vartheta)$ [**L. 20, 21]**. In these considerations, synovial fluid density variations are neglected, i.e. incompressible liquid is considered. In the aforementioned equations the known dependence was used between interfacial energy γ and the exponent of hydrogen ion concentration p_H and cartilage surface wettability *We* **[L. 22]**. The influences of electrostatic field on the viscosity of synovial fluid are taken into account [**L.23]**. We apply boundary layer simplifications in the abovementioned system of hydrodynamic equations, i.e. we neglect the terms of the order of radial clearance equal to value 10^{-4}. After calculations and term ordering, we determine the system of hydrodynamic lubrication equations for the phospholipid bilayer in a stochastic form [**L. 5]** and the expected random solutions: hydrodynamic pressure, temperature and three synovial fluid components [**L. 4]**.

An outline of half-analytical as well as numerical solutions of the system of the

aforementioned hydrodynamic equations mainly concerns stochastic and non-stochastic (excluding operator *EX*) non-linear partial differential integral hydrodynamic equations for two spherical surfaces [**L. 5]**. In a particular case, numerical calculations are elaborated for the equation determining two-dimensional hydrodynamic pressure p as well as an equation that describes three-dimensional temperature distribution T. These equations are always mutually coupled through the three-dimensional dynamic viscosity function η_T variable in the direction of the gap height and dependent on temperature [**L. 5]**. The results of the calculations are applied in the problem presented in this paper.

BRIEF DESCRIPTION OF MEASUREMENTS

Using AFM, we have measured the real probability density function f of random gap height change for spherical hip joint, for spherical cartilage surfaces occurring in human hip joint see Appendix 1. We have considered the expected values m of gap height and standard deviations σ, to apply in this paper concrete estimation intervals of analytical bio-tribology parameters for considered surface. Experimental measurement [**L. 4]** and [**L. 5]** of mentioned joints gap height with radial clearance ε_0 from 2 to 10μm have proved that the dimensionless random variable of corrections for gap height, marked with the symbol δ_1, is most often manifested by two characteristic types of probability density functions [**L. 4–5]**. These are symmetrical and anti-symmetrical functions. Symmetrical density functions f_s of correction parameters for spherical hip joint surfaces occur much less frequently than anti-symmetrical functions (about 12 times in 100 measurements with a probability of P_s = 0.12). They are characterized by a symmetric distribution of random probability changes in term of gap height increases and decreases. In this case, probabilities of random increases in joint height gap are equal to the probabilities of random decreases [**L. 5]**.

Among the frequently occurring unsymmetrical correction parameter, the density functions describing random increases and decreases in gap height, we generally have two types of functions. The first type concerns function f_N, where the probabilities of random gap height increases dominate over the probabilities of random gap height decreases **[L. 4–5]**. The second type concerns function f_n, where the probabilities of random gap height decreases dominate over the probabilities of random gap height increases. Both functions f_N, f_n are considered for gap height restricted between human hip joint surfaces. There are two cases for anti-symmetrical probability density distribution functions f_N, and each one of them occur 22 times in 100 measurements with probability P_N = 0,22. For the next two cases for anti-symmetrical probability density distribution functions f_n, each one of them occur 22 times in 100 measurements with probability P_n = 0.22. The measurement multiplicity, equal to 12+2×22+2×22 = 100, creates a probabilistic complete system of events **[L. 4–5, 18]**.

For the symmetrical function shown in **Fig. A1**, expected value m_S = 0 for the random variable of gap height corrections was determined from Formula (2). The standard deviation determined from Formula (3) produces the following value: σ_S = 0.4082. The standard deviation interval was superimposed onto **Fig. A1** on upper horizontal axis δ_1. In this interval, due to random changes for the measurements conducted, the random expected value of increases and decreases in the gap height may change its location. The changes are assigned a change value of the entire gap, which is read from lower horizontal axis $1+\delta_1$, where the dimensionless gap height that is equal to 1 is assigned to value correction δ_1 = 0 on the upper horizontal axis. Thus, the standard deviation interval and the expected function values of the dimensional height of the entire gap varies in the range of the following **[L. 4–5]**:

$$(m_S - \sigma_S, m_S + \sigma_S) = (-0.4082, +0.4082), \quad (4a)$$

$$0.5918 \times \varepsilon_T(\delta_1 = 0) < EX(\varepsilon_T) < 1.4082 \times \varepsilon_T(\delta_1 = 0), \quad (4b)$$

where gap height $\varepsilon_T(\delta = 0) \equiv \varepsilon_0 \varepsilon_{T1s}(\varphi, \vartheta_1) = \varepsilon_T(\varphi, \vartheta_1, \delta_1 = 0)$. The height of the entire gap may decrease or increase. Such changes in gap height occur with a probability from P_s = 0.5918 to P_s = 1.0000, indicated on the vertical axis in **Fig. A1**.

Figure A2a, b, c, d that presents unsymmetrical functions f_N, f_n are shown the following expected values for the random variable of gap height corrections for spherical surfaces determined from Formula (2): m_N = +0.125; m_N = +0.250, m_n = –0.250; m_n = –0.125. The standard deviations of the random variable of corrections determined from Formula (3) produce the following values: σ_N = 0.3886, σ_N = 0.3818, σ_n = 0.3818, and σ_n =

0.3886. The standard deviation intervals of the random variable of corrections $(m_N-\sigma_N,\ m_N+\sigma_N)$, $(m_n-\sigma_n,\ m_n+\sigma_n)$ were superimposed onto **Figs. A2a, b, c, d** on axis δ_1. In this interval, due to random changes, the random expected value of increases and decreases in the gap height may change its location. The changes are assigned a change value of the entire gap, which is read on collinear second horizontal axis $1+\delta_1$. Thus, the standard deviations intervals and the expected function values of the dimensional height of the entire gap for spherical surfaces vary in the following ranges:

$$(-0.2636, +0.5136);\ (-0.1918, +0.6318);\ (-0.6318, +0.1318);\ (-0.5136, +0.2636). \quad (5a)$$

$$\begin{gathered}0.7364\times\varepsilon_T(\delta_1=0)<EX(\varepsilon_T)<1.5136\times\varepsilon_T(\delta_1=0),\\ 0.8682\times\varepsilon_T(\delta_1=0)<EX(\varepsilon_T)<1.6318\times\varepsilon_T(\delta_1=0),\\ 0.3682\times\varepsilon_T(\delta_1=0)<EX(\varepsilon_T)<1.1318\times\varepsilon_T(\delta_1=0),\\ 0.4864\times\varepsilon_T(\delta_1=0)<EX(\varepsilon_T)<1.2636\times\varepsilon_T(\delta_1=0).\end{gathered} \quad (5b)$$

Changes in the gap height occur successively with probabilities from $P_N = 0.6046$ through $P_N = 0.7884$, $P_N = 0.9166$ to $P_N = 1.0000$ indicated on the vertical axis in **Figs. A2a ,b,** similarly as with the P_n probabilities in **Figs. A2c, d**. Based on the conclusions from the studies illustrated in **Figs. A1, A2 a, b, c, d**, the following final forms of the expected values of the lower and upper limits of the standard deviation interval of the gap height between spherical hip surfaces *(h),* the value of the expected function of the spherical *(h)* joint gap height, the speed of synovial fluid, and its viscosity change together with probability: $0.6708 \le P \le 1.0000$ in the following random value intervals are presented **[L. 4–5, 18]:**

$$\begin{gathered}0.6120\ \varepsilon_T(\delta_1=0) = (1+m^h-\sigma^h)\ \varepsilon_T(\delta_1=0) \le EX(\varepsilon_T)\\ \le(1+m^h+\sigma^h)\varepsilon_T(\delta_1=0) = 1.3879\ \varepsilon_T(\delta_1=0),\end{gathered} \quad (6a)$$

$$\begin{gathered}0.7205\ \nu(\delta_1=0) = (1+m^h+\sigma^h)^{-1}\nu(\delta_1=0) = \le EX(\nu)\\ \le(1+m^h-\sigma^h)^{-1}\nu(\delta_1=0) = 1.6339\nu(\delta_1=0),\end{gathered} \quad (6b)$$

$$\begin{gathered}0.6120\eta_T\ (\delta_1=0) = (\ 1+m^h-\sigma^h)\ \eta_T\ (\delta_1=0) \le EX(\eta_T)\\ \le(1+m^h+\sigma^h)\eta_T\ (\delta_1=0) = 1.3879\ \eta_T\ (\delta_1=0).\end{gathered} \quad (6c)$$

RANDOM BIO-TRIBOLOGY PARAMETERS AND ITS LOCALIZATION

Random load carrying capacity fractions

By virtue of the density function, measurements described in **Appendix, Fig. A2a, b** and in Section 3, after analytical, numerical Mathcad 15 Professional Program calculations for two kinds of phospholipids PS and PC, the following results were obtained that present the random load carrying capacity quotients in **Figs. 3a, 3b**. The dimensionless capacity random quotient ξ_C depicted in the vertical axis in **Fig. 3a** denotes the fraction of the capacity of random effects (nominator) to the capacity without random effects (the denominator).

For f_N – density function (random increments dominate over decrements), we demonstrate in **Fig. 3a** that the quotient ξ_C of the dimensionless load carrying capacity attains a decrement value of 0.558 for PS, PC with probability $P = 0.604$, and it attains an increment value 2.393 with probability $P = 0.729$ for PS and with probability $P = 0{,}788$ for PC, in comparison with dimensionless quotient $\xi_C = 1$, obtained without any random changes for $\delta_1 = 0$.

Inside the standard deviation interval on axis δ_1, we find the following expected value: $m_1 = 0.25$ for the corrected gap height $(m_1+1)\cdot\varepsilon_T = 1.25\varepsilon_T$, where the expected dimensionless capacity quotient attains an increment of 1.55 with probability $P = 0.916$ for PC in comparison with capacity quotient $\xi_C = 1$,without any random effects **[L. 24]**. We find the expected value: $m_2 = 0.125$ for the corrected gap height $(m_2+1)\cdot\varepsilon_T = 1.125\varepsilon_T$, where the expected dimensionless capacity quotient attains an increment of 1.34 with probability $P = 0.937$ for PS, in comparison with the dimensionless capacity quotient without any random effects for $\xi_C = 1$.

For density function f_N, **Fig. 3b** demonstrates that in a radial clearance interval from 2 μm to 10 m, the dimensionless expected value of capacity quotient ξ_C, decreases from 1.55 to 1.50 with constant probability $P = 0.916$ and constant expected value of gap height $(m_1+1)\ \varepsilon_T = 1.25\varepsilon_T$ for PC. Moreover, the capacity quotient ξ_C = decreases from 1.34 to 1.31 with constant probability $P = 0.937$ and constant expected value of gap height $(m_2+1)\ \varepsilon_T = 1.125\varepsilon_T$ for PS, in comparison with the dimensionless capacity quotient without any random effects for $\xi_C = 1$.

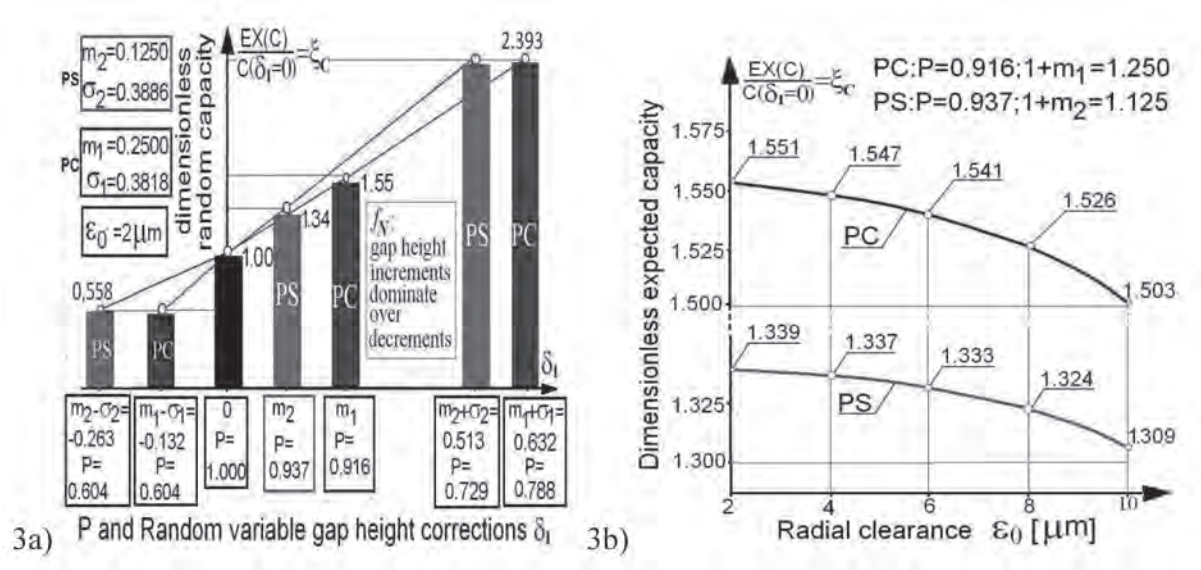

Fig. 3. Dimensionless random capacity quotient ξ_C for spherical surface after random density function f_N: a) versus random variable gap height corrections δ_1 and probability P, inside the standard deviation interval of gap height with radial clearance 2 μm, b) versus radial clearance from 2 to 10 μm, with constant probability P and constant expected value of gap height for PC and PS

Rys. 3. Bezwymiarowe ilorazy losowej siły nośnej ξ_C dla powierzchni sferycznych oraz losowych gęstości f_N: a) jako funkcja losowo zmiennych korekt wysokości szczeliny δ_1 i prawdopodobieństwa P wewnątrz przedziału odchylenia standardowego wysokości szczeliny przy luzie promieniowym 2 μm, b) jako funkcja luzu promieniowego od 2 do 10 μm, o stałym prawdopodobieństwie P i o stałej wartości oczekiwanej wysokości szczeliny dla PC oraz PS

Random friction coefficient fractions

By virtue of the density function, measurements described in **Appendix, Figures A2a, b** and in Section 3, once analytical, numerical Mathcad 15 Professional Program calculations for two kinds of phospholipids PS and PC had been performed, the following results were obtained presented the random quotients of friction coefficients in **Figs. 4a, 4b**.

The dimensionless friction coefficient random quotient ξ_μ depicted in the vertical axis in **Fig. 4a** denotes the fraction of friction coefficient of random effects (nominator) to the friction coefficient without any random effects (denominator).

For f_N – density function, **Fig. 4a** demonstrates that quotient ξ_μ of the dimensionless friction coefficient attains a decrement value of 0.344 for PS and PC with probability $P = 0.604$, and it attains an increment value of 2.272 with probability $P = 0.729$ for PS and with probability $P = 0{,}788$ for PC, in comparison with dimensionless quotient $\xi_C = 1$ obtained without random changes. Inside the standard deviation interval on axis δ_1, we find the following expected value: $m_1 = 0.25$ for the corrected gap height $(m_1+1) \cdot \varepsilon_T = 1.25\varepsilon_T$, where the expected dimensionless friction coefficient quotient attains an increment of 1.50 with probability $P = 0.916$ for PC in comparison with friction coefficient quotient $\xi_\mu = 1$, without random effects. And we find the following expected value: $m_2 = 0.125$ for the corrected gap height $(m_2+1) \cdot \varepsilon_T = 1.\,125\varepsilon_T$, where the expected quotient of the friction coefficient attains an increment of 1.31 with probability $P = 0.937$ for PS in comparison with friction coefficient quotient $\xi_\mu = 1$ without random effects.

For density function f_N, **Fig. 4b** demonstrates that in a radial clearance interval from 2 μm to 10 μm, the dimensionless quotient ξ_μ of the expected value friction coefficient decreases from 1.50 to 1.35 with constant probability $P = 0.916$ and constant expected value of gap height $(m_1+1)\ \varepsilon_T = 1.25\varepsilon_T$ for PC. Moreover, quotient ξ_μ decreases from 1.31 to 1.22 with constant probability $P = 0.937$ and the constant expected value of gap height $(m_2+1)\ \varepsilon_T = 1.125\varepsilon_T$ for PS in comparison with the dimensionless friction coefficient quotient without random effects for $\xi_\mu = 1$.

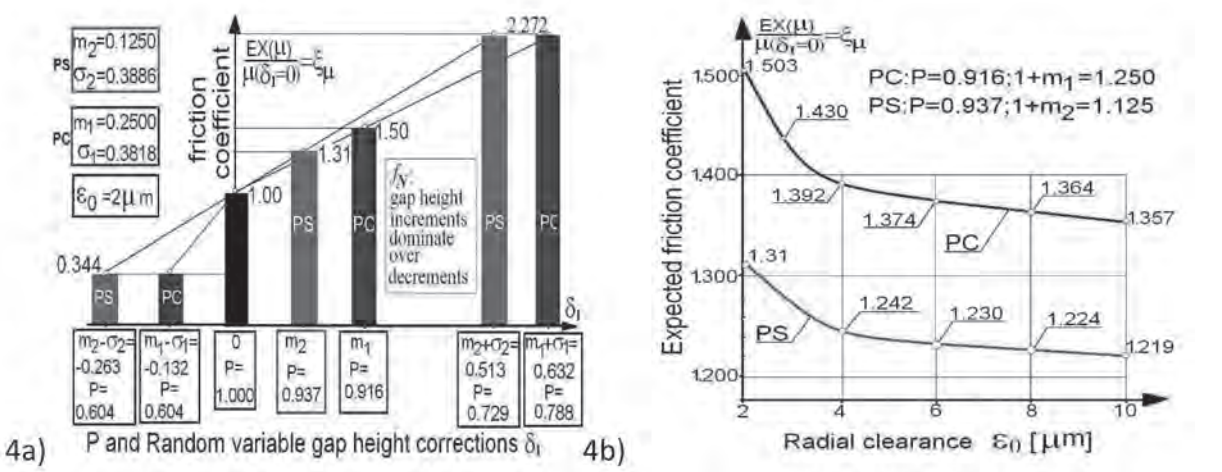

Fig. 4. Dimensionless random friction coefficient quotients ξ_μ for spherical surfaces and random densities f_N: a) as a function of random variable gap height corrections δ_1 and probability P inside the standard deviation interval of the gap height with radial clearance 2 μm, b) as a function of radial clearance from 2 to 10 μm, with constant probability P and constant expected value of gap height for PC and for PS

Rys. 4. Bezwymiarowe ilorazy losowych współczynników tarcia ξ_μ dla powierzchni sferycznych oraz losowych gęstości f_N: a) jako funkcja losowo zmiennych korekt wysokości szczeliny δ_1 i prawdopodobieństwa P wewnątrz przedziału odchylenia standardowego wysokości szczeliny przy luzie promieniowym 2 μm; b) jako funkcja luzu promieniowego od 2 do 10 μm, o stałym prawdopodobieństwie P i o stałej wartości oczekiwanej wysokości szczeliny dla PC oraz dla PS

By virtue of the density function, measurements described in **Appendix, Figures A2 c, d,** for density function f_n (random decrements dominate over increments), we have for PS the following: expected value $m_2 = -0.125$, and the corrected value of gap height $0.875\varepsilon_T$. For PC, we have the expected value $m_1 = -0.25$, the corrected value of gap height $0.75\varepsilon_T$. Increases and decreases of the expected capacity and friction coefficient values for density functions f_N and f_n are similar.

Random fraction of dynamic viscosity

By virtue of the density function, measurements described in **Appendix, Figures A2a, b** and Section 3, once analytical and numerical Mathcad 15 Professional Program calculations for two kinds of phospholipids PS and PC had been performed, the following results were obtained presented as the random variations of synovial fluid dynamic viscosity in **Figs. 5a, 5b.**

The dimensionless dynamic viscosity random quotient ξ_η, which is depicted on the vertical axis in **Fig. 5a,** denotes the fraction of dynamic viscosity random effects (a nominator) to the dynamic viscosity without random effects (a denominator).

For f_N – density function (random increments dominate over decrements), **Fig. 5a** shows that the quotient ξ_η of the dimensionless dynamic viscosity attains a decrement of 0.612 for PS and PC with probability P = 0.604, and it attains an increment of 1.388 with probability P = 0.729 for PS and with probability P = 0.788 for PC, in comparison to dimensionless viscosity quotient $\xi_\eta = 1$, obtained without random changes. Inside the standard deviation interval on axis δ_1, we find the following expected value: $m_1 = 0.25$ for corrected gap height $(m_1+1) \cdot \varepsilon_T = 1.25\varepsilon_T$, where the expected dynamic viscosity quotient increments attain a value of 1.15 with probability P = 0.916 for PC, in comparison with dynamic viscosity quotient ξ_η = 1, without random effects. And we find the following expected value: $m_2 = 0.125$ for corrected gap height $(m_2+1) \cdot \varepsilon_T = 1.\ 125\varepsilon_T$, where the increments of the expected dynamic viscosity quotient attain a value of 1.09 with probability P = 0.937 for PS, in comparison with the dynamic viscosity quotient without random effects for $\xi_\eta = 1$.

For density function f_N, **Fig. 5b** demonstrates that in the radial clearance interval from 2 μm to 10 μm, the dimensionless random quotient ξ_η of the expected value for bio-fluid dynamic viscosity increases from 1.15 to 1.19 with constant probability $P = 0.916$ and a constant expected value of gap height $(m_1+1)\ \varepsilon_T = 1.25\varepsilon_T$ for PC. Moreover,

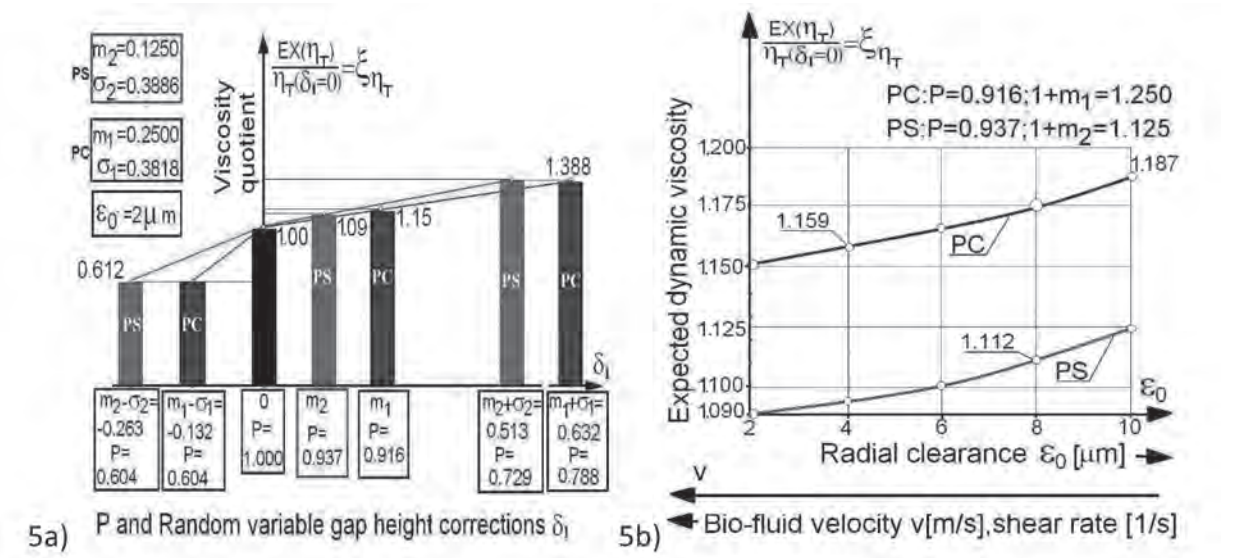

Fig. 5. Dimensionless random dynamic viscosity quotients ξ_η for spherical surfaces and random densities f_N: a) as a function of random variable gap height corrections δ_1 and probability P inside the standard deviation interval of gap height with radial clearance 2 μm, b) as a function of radial clearance from 2 to 10 μm, with constant probability P and constant expected value of gap height for PC and for PS

Rys. 5. Bezwymiarowe ilorazy losowych wartości lepkości dynamicznej ξ_η biocieczy dla powierzchni sferycznych oraz losowych gęstości f_N: a) jako funkcja losowo zmiennych korekt wysokości szczeliny δ_1 i prawdopodobieństwa P wewnątrz przedziału odchylenia standardowego wysokości szczeliny przy luzie promieniowym 2 μm, b) jako funkcja luzu promieniowego od 2 do 10 μm, o stałym prawdopodobieństwie P i o stałej wartości oczekiwanej wysokości szczeliny dla PC oraz dla PS

the random quotient ξ_η increases from 1.09 to 1.13 with constant probability P = 0.937 and constant expected value of gap height $(m_2+1)\,\varepsilon_T = 1.125\varepsilon_T$ for PS, in comparison with the dimensionless dynamic viscosity quotient without random effects for $\xi_\eta = 1$.

Comparison of random variations

The increase of the absolute values of negative $\delta_1 < 0$ (positive $\delta_1 > 0$) gap height corrections δ_1 implies probability P decrements of random quotient ξ_C, ξ_μ, ξ_η (see the horizontal axis in **Figs. 3a, 4a, 5a,** respectively).

The negative (positive) values of gap height corrections δ_1 on the left (right) side on the horizontal axis in **Figs. 3a, 4a, 5a** denote random decrements (increments) of the gap height, respectively.

On the horizontal axis in **Figs. 3a, 4a, 5a** for gap height density function f_N, the dimensional standard deviation interval of the gap height is depicted in the form: $(1+m_2-\sigma_2 < 1+m_2+\sigma_2)\,\varepsilon_T$, i.e. $(0.7364\ ,1.5136)\cdot\varepsilon_T$ for PS with standard deviation $\sigma_2 = 0.3880$, and $(1+m_1-\sigma_1 < 1+m_1+\sigma_1)\,\varepsilon_T$, i.e. $(0.8614, 1.6386)\cdot\varepsilon_T$ for PC, with standard deviation $\sigma_1 = 0.3818$. For gap height density function f_n, the abovementioned standard deviation interval of the gap height are as follows: $(0.4932 < 1.2568)\cdot\varepsilon_T$, for PS, and $(0.3682 < 1.1318)\cdot\varepsilon_T$ for PC.

The probabilities of the decrements of dimensionless quotients ξ_C, ξ_μ, ξ_η, of the capacity, the friction coefficient and the dynamic viscosity variation presented in **Figs. 3a, 4a, 5a** are relatively smaller than the probabilities of the increments of the aforementioned quotients.

On the horizontal axis in **Figs. 3b, 4b, 5b** dimensional radial clearances ε_0 are depicted from 2 to 10 micrometres for the spherical surface of the human hip joint. It is evident that the quotient of the expected capacity and friction coefficient decrease for radial clearance increments (see **Figs. 3b, 4b**). However, **Fig. 5b** shows an increase of the quotient of the expected dynamic viscosity value versus radial clearance increments (see **Fig. 5b**). This fact can be explained by virtue of the fluid mechanics law. The radial clearance increments imply the decrements of the velocity and the shear rate of the non-Newtonian bio-fluid flow in the gap of the human hip joint. On the grounds of non-Newtonian pseudo-plastic synovial fluid flows, it may be concluded that shear rate decrements during the flow imply dynamic viscosity increments. This fact completes this phenomenon.

CONCLUSIONS

Stochastic and expected values of the synovial fluid dynamic viscosity in the human hip joint, ones that occur in standard deviation regions of the random values of gap height, increase ca. from 9 to 12 per cent for PS and from 15 to 19 per cent for PC additions versus radial clearance increments from 2 to 10 micrometres in comparison with the dynamic viscosity quotient without random effects.

The expected random values of the load carrying capacity in the human hip joint that occur in standard deviation regions of the gap height decrease from 34 to 31 per cent for PS-and from 55 to 50 per cent for PC additions, versus radial clearance increments from 2 to 10 micrometres, in comparison with the dynamic viscosity quotient without random effects.

The expected random values of the friction coefficient in the human hip joint that occur in standard deviation regions of the gap height decrease about from ca. 31 to 22 per cent for PS-and from 50 to 3 per cent for PC additions, versus radial clearance increments from 2 to 10 micrometres, in comparison with the dynamic viscosity quotient without random effects.

Random expected values of synovial fluid dynamic viscosity, the load carrying capacity and the friction coefficient in the human hip joint localize in a standard deviation interval of the gap height from $0.875\varepsilon_T$ to $1.125\varepsilon_T$ with probability P = 0.937 for PS and from $0.75\varepsilon_T$ to $1.255\varepsilon_T$ with probability P = 0.916 for PC.

DISCUSSION

The presented paper describes the flow of synovial fluid with non-Newtonian properties in a biological gap between two isotonic, curvilinear, rotational spherical surfaces with PL bilayer, susceptible to deformations caused by, among others, random changes, roughness geometry, stochastic loading of the surface, as well as genetic and volumetric growth of living articular tissue. The concept of iso-osmosis or isotonic flow defines layers of biological cartilage surfaces with PL remaining in osmotic balance with respect to each other. Isotonic, impermeable biological membranes include, among others, a lipid bilayer, which eliminate flow across the layer. The exception may be nanometre channels transporting certain types of liquid **[L. 4]**.

The present work demonstrates the influence of the physical properties of articular tissue with a phospholipid bilayer and a random gap height on the viscosity of synovial fluid in the area of the boundary layer of the surface flowed around. According to the author, the influence of the physical properties of flowed around biological surfaces on the viscosity of the fluid in the boundary layer will even be more visible in lamellar flows, where the gap height reaches a value of ca. 2–3 nm, i.e. the order of the thickness of the PL membrane. In accordance with the author's suggestion, the aforementioned random variations of the gap height and its influences on velocity and viscosity changes will be measurable and comparable if we are going to apply machine vision systems with image analysis **[L. 25]**.

The research enables the determination of the standard deviation intervals of the gap height, including the localization of the expected values of tribology parameters. The aforementioned localization depends on the probability of random values for bio-fluid dynamic viscosity, hydrodynamic pressure, frictional forces, and the coefficients of friction. Based on the experimental study of random gap height corrections of cooperating spherical cartilage surfaces and the random density function, we obtain large or small intervals of estimations for the expected values of the abovementioned bio-tribology parameters. For example, a small interval of changes in expected values, seemingly favourable, but with low probabilities of occurrence, is much less useful than a large interval of changes in the expected values of a given parameter with high and low probabilities of occurrence, enabling an assignment of the expected value to the highest possible probabilities of occurrence.

APPENDIX

After the completion of AFM measurements, the symmetrical of density function f_s for spherical surfaces *(h)* is shown in **Fig. A1**.

The two types of unsymmetrical correction parameter density functions that describe random increases and decreases in the gap height for spherical surfaces are presented in **Figs. A2a, b** and in **Figs. A2c, d**.

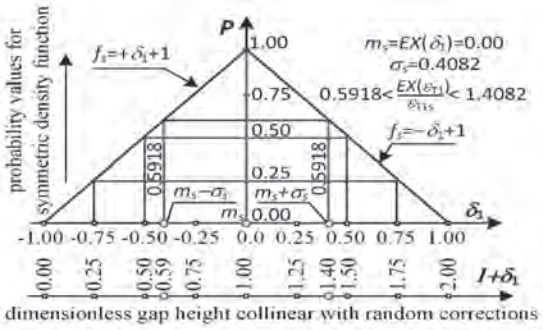

$$f_S(\delta_1) \equiv \begin{cases} 1+\delta_1 & for \quad -1 \le \delta_1 \le 0, \\ 1-\delta_1 & for \quad 0 \le \delta_1 \le 1, \\ 0 & for \quad |\delta_1| > 1. \end{cases}$$

Fig. A1. The expected value m_s and standard deviation σ_s of the hip gap height depicted on the symmetrical probability density function f_s with a vertical axis of probability P, where the upper horizontal axis gives dimensionless values of the random variable of corrections δ_1 of increases and decreases in joint gap height, the lower horizontal axis indicates the dimensionless height of the entire gap $1+\delta_1$ (Figures elaborated after Authors own measurements and studies)

Rys. A1. Wartość oczekiwana m_s oraz odchylenie standardowe σ_s dla wysokości szczeliny pokazane na symetrycznym rozkładzie funkcji gęstości prawdopodobieństwa f_s z osią pionową dla rzędnych prawdopodobieństwa P, z górną osią poziomą o bezwymiarowych wartościach wzrostów i spadków zmiennych losowo korekt δ_1 wysokości szczeliny oraz z dolną poziomą osią skalującą bezwymiarowe wartości całej wysokości szczeliny $1+\delta_1$ (rysunek wykonany na podstawie własnych pomiarów i badań autorów)

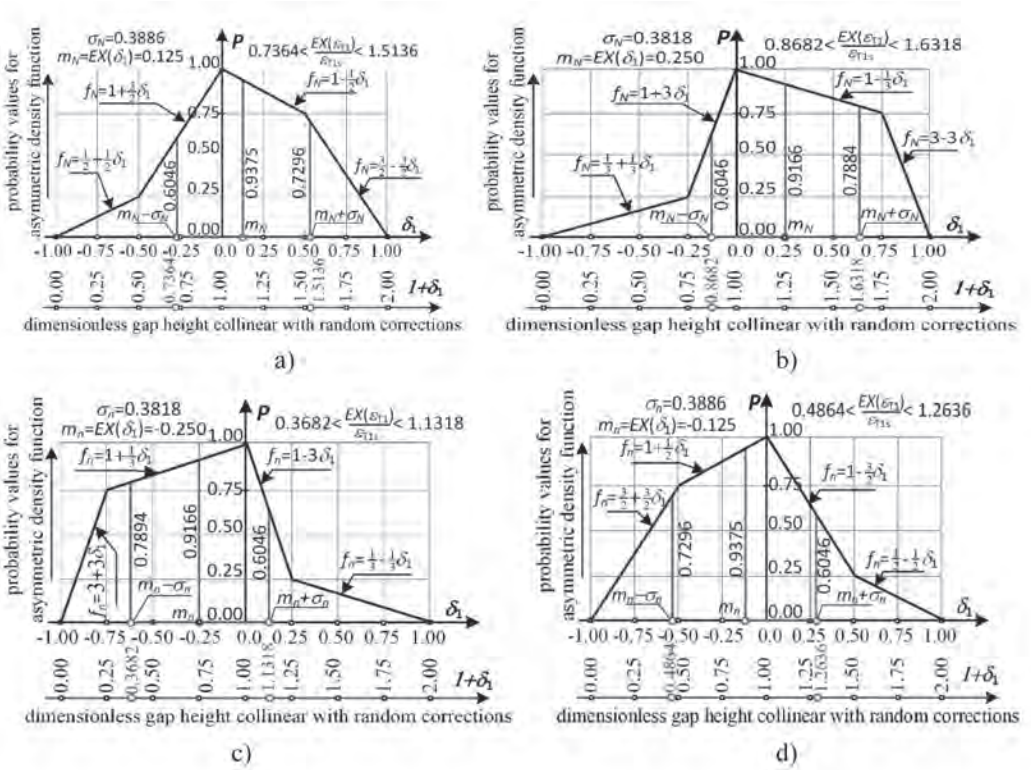

Fig. A2. The expected values m_N, m_n and standard deviations σ_N, σ_n of the hip gap height depicted on the anti-symmetrical probability density functions: a), b) f_N for dominance of random increases over decreases of joint gap height, c), d) f_n for dominance of random decreases over random increases of joint gap height; where the vertical axis indicates probabilities P, the upper horizontal axis gives dimensionless values of the random variable of increase and decrease corrections of joint gap height δ_1, the lower horizontal axis indicates the heights of the entire gap $1+\delta_1$ (Figures elaborated after Authors own studies)

Rys. A2. Wartości oczekiwane m_N, m_n oraz odchylenia standardowe σ_N, σ_n dla wysokości szczeliny pokazane na symetrycznych rozkładach funkcji gęstości prawdopodobieństwa: a), b) f_N, gdy losowe wzrosty wysokości szczeliny dominują nad ubytkami, c), d) f_n, gdy losowe ubytki wysokości szczeliny dominują nad wzrostami: w obu przypadkach z osią pionową dla rzędnych prawdopodobieństwa P, z górną osią poziomą o bezwymiarowych wartościach wzrostów i spadków zmiennych losowo korekt δ_1 wysokości szczeliny oraz z dolną poziomą osią skalującą bezwymiarowe wartości całej wysokości szczeliny $1+\delta_1$ (rysunek wykonany na podstawie własnych pomiarów i badań autorów)

REFERENCES

1. Andersen O.S., Roger E., et.al.: Bilayer thickness and Membrane Protein Function: An Energetic Perspective, "Annular Review of Biophysics and Biomolecular Structure" 2014, 36 (1), pp. 107–130.
2. Bhushan B.: Handbook of Micro/Nano Tribology, second ed. CRC Press, Boca Raton, London, New York, Washington D.C. 1999.
3. Bhushan B.: Nanotribology and nanomechanics of MEMS/NEMS and BioMEMS/BioNEMS materials and devices, "Microelectronic Engineering" 2007, 84, pp. 387–412.
4. Wierzcholski K.: A New Progress in Random Hydrodynamic Lubrication for Movable Non-Rotational Curvilinear Biosurfaces with Phospholipid Bilayers, Lidsen Publishing Inc, Recent Progress in Materials, 2021, volume 3, issue 2, p.1-38doi:10.21926/rpm.2102023, http://www.lidsen.com/journals/rpm/rpm-03-02-023.
5. Wierzcholski K., Miszczak A.: Estimation of Random Bio-Hydrodynamic Lubrication Parameters for Joints with Phospholipid Bilayers, "Bulletin of Polish Academy of Sciences Technical Sciences" vol. 69 (1) e135834, DOI:10.24425/bpasts. 2021.135834.
6. Cwanek J.: The usability of the surface geometry parameters for the evaluation of the artificial hip joint wear. Rzeszów University Press, Rzeszów 2009.
7. Mow V.C., Ratcliffe A., Woo S.: Biomechanics of Diarthrodial Joints, Springer Verlag, Berlin–Heidelberg New York 1990.
8. Wierzcholski K.: Time depended human hip joint lubrication for periodic motion with stochastic asymmetric density function, "Acta of Bioengineering and Biomechanics", 2014 16 (1), pp. 83–97.
9. Chagnon G., Rebouah M., Favier D.: Hyper-elastic Energy Densities for Soft Biological Tissues: A Review. "Journal of Elasticity" 2015 Aug., 120 (2), pp. 129–160.
10. Gadomski A., Bełdowski P., Miguel Rubi J., Urbaniak W., Wayne K., Auge W.K., Holek I.S., Pawlak Z.: Some conceptual thoughts toward nano-scale oriented friction in a model of articular cartilage, "Mathematical Biosciences" 2013, 244, pp. 188–200.
11. Hills B.A.: Oligolamellar lubrication of joint by surface active phospholipid, "Journal of Reumatology" 1989, 16, pp. 82–91.
12. Hills B.A.: Boundary lubrication in vivo, "Proc. Inst. Mech. Eng. Part H: J. Eng. Med." 2000, 214, pp. 83–87.
13. Marra J., Israelachvili J.N.: Direct measurements of forces between phosphatidylcholine and phosphatidylethanolamine bilayers in aqueous electrolyte solutions, "Biochemistry" 1985, 24, pp. 4608–4618.
14. Schwarz I.M., Hills B.A.:Synovial surfactant: Lamellar bodies in type B synoviocytes and proteolipid in synovial fluid and the articular lining, "British Journal of Rheumatology" 1966, 35 (9), pp. 821–827.
15. Pawlak Z., Urbaniak W., Hagner-Derengowska M.W.: The Probable Explanation for the Low Friction of Natural Joints, "Cell Biochemistry and Biophysics" 2015, 71 (3), pp. 1615–1621.
16. Wierzcholski K., Miszczak A.: Mathematical principles and methods of biological surface lubrication with phospholipids bilayers, 2019, www.elsevier.com.Biosystems, https://doi.org/10.1016/j.biosystems.2018 11,002.
17. Petelska A.D., Figaszewski Z.A.: Effect of pH on interfacial tension of bilayer lipid membrane, "Biophysical Journal" 2000, 78, pp. 812–817.
18. Fisz M.: Rachunek prawdopodobieństwa i statystyka matematyczna, PWN, Warszawa 1958.
19. Wierzcholski K., Miszczak A.: Electro-Magneto-Hydrodynamic Lubrication, "Open Physics" 2018, 16 (1), pp. 285–291.
20. Wierzcholski K.: Joint cartilage lubrication with phospholipids bilayer, "Tribologia" 2016, 2 (265), pp. 145–157.
21. Wierzcholski K.: Topology of calculating pressure and friction coefficients for time-dependent human hip joint lubrication, "Acta of Bioengineering and Biomechanics" 2011, 13 (1), pp. 41–56.
22. Pawlak Z., Petelska A.D., Urbaniak W., Fusuf K.Q., Oloyede A.: Relationship Between Wettability and Lubrication Characteristics of the Surfaces of Contacting Phospholipids-Based Membranes, "Cell Biochemistry and Biophysics" 2012, 65 (3), pp. 335–345.
23. Syrek P.: Analiza parametrów przestrzennych aplikatorów małogabarytowych, wykorzystywanych w magnetoterapii. AGH University of Sciences and Technology, Kraków 2010, doctor thesis.
24. Pawlak Z., Figaszewski Z.A., Gadomski A., Urbaniak W., Oloyede A.: The ultra–low friction of the articular surface is pH-dependent and is built on a hydrophobic underlay including a hypothesis on joint lubrication mechanism, "Tribology International" 2010, 43, pp. 1719–1725.
25. Gospodarczyk J. et all: Estimating Vehicle Speed Based on Image Camera, "Health and Sport" 2016; 6(4):122-126,doi.http://dx.doi.org/10.5281/zenodo.49880, http://ojs.ukw.edu.ol/index.php/johs/article/view/3456.